Characteristics of charge and discharge of PMMA samples due to electron irradiation*

Feng Guo-Bao(封国宝)[a], Wang Fang(王 芳)[a)†], Hu Tian-Cun(胡天存)[b)], and Cao Meng(曹 猛)[a)]

[a)] *Key Laboratory for Physical Electronics and Devices of the Ministry of Education, Department of Electronic Science and Technology, Xi'an Jiaotong University, Xi'an* 710049, *China*

[b)] *National Key Laboratory of Science and Technology on Space Microwave, Xi'an* 710000, *China*

(Received 12 May 2015; revised manuscript received 4 June 2015; published online 12 October 2015)

In this study, using a comprehensive numerical simulation of charge and discharge processes, we investigate the formation and evolution of negative charge and discharge characteristics of a grounded PMMA film irradiated by a non-focused electron beam. Electron scattering and transport processes in the sample are simulated with the Monte Carlo and the finite-different time-domain (FDTD) methods, respectively. The properties of charge and discharge processes are presented by the evolution of internal currents, charge quantity, surface potential, and discharge time. Internal charge accumulation in the sample may reach saturation by primary electron (PE) irradiation providing the charge duration is enough. Internal free electrons will run off to the ground in the form of leakage current due to charge diffusion and drift during the discharge process after irradiation, while trapped electrons remain. The negative surface potential determined by the charging quantity decreases to its saturation in the charge process, and then increases in the discharge process. A larger thickness of the PMMA film will result in greater charge amount and surface potential in charge saturation and in final discharge state, while the electron mobility of the material has little effects on the final discharge state. Moreover, discharge time is less for smaller thickness or larger electron mobility. The presented results can be helpful for estimating and weakening the charging of insulating samples especially under the intermittent electron beam irradiation in related surface analysis or measurement.

Keywords: charge and discharge, PMMA, numerical simulation, electron irradiation

PACS: 79.20.Ap, 72.20.Dp, 02.70.Uu, 72.80.Le **DOI:** 10.1088/1674-1056/24/11/117901

1. Introduction

Charging phenomenon and related effects of various insulating samples due to electron beam (e-beam) irradiation have been attracting a great deal of attention since they were first observed in the scanning electron microscope (SEM) to distort images in 1960s.[1,2] Charging of specimen may not only degrade the accuracy of e-beam microanalysis, but also reduce dimension metrology and lithography.[3–8] On the other hand, the accumulated internal charges will discharge by leaking to the grounded basement in the way of charge transport resulting from the internal built-in E-field and the charge density gradient.[9–11] Hence, discharge presented by leakage current during the intermittence of electron irradiation will weaken charging effects. This occurrence of charge and discharge has significance in application fields of micromachining, space environment, and so on.[12–15] Therefore, it is important to understand characteristics of combinational charge and discharge processes for reducing impacts of charging effects.

Charge as a result of e-beam irradiation and the subsequent discharge are related to the interaction between electrons and samples, and charge transport. Charging is caused by the imbalance between the inflow current, i.e., primary electron (PE) current, and the outflow currents, i.e., secondary electron (SE) and leakage electron currents. Due to the interruption of PEs, both PE and SE currents are absent, and only the leakage current continues during the discharge process.[16] Then, charge and discharge processes have intrinsic interrelation and dependence on parameters of electron irradiation and samples. Theoretical studies have simulated the charge process to obtain transient surface potential using radiation-induced conductivity (RIC) method with ignoring effects of SE emissions due to PE scattering and dynamic charging in the sample.[17–20] Combining with Geant4 used in electron scattering, the RIC method is still appropriate on charge up effects in the space environment of high-energy (MeV) e-beam irradiation.[21] Some other works simulating PE scattering in insulator films with Monte Carlo (MC) method present the dynamic charging effect on SE emission during the charge process,[22,23] showing the influence of SE emission on charge. Meanwhile, experimental researches usually examined currents and charge quantity of the PMMA film with certain sample parameters during charge and discharge processes under intermittent e-beam irradiation.[16,17,24] There still lacks studies concerning effects of related sample parameters on both charge and discharge characteristics, probably due to the difficulty in continuously changing the sample parameters in experiments. Therefore, a comprehensive simulation considering the scattering of PEs

*Project supported by the National Natural Science Foundation of China (Grant Nos. 11175140 and 11004157) and the Foundation of National Key Laboratory of Space Microwave Technology of China (Grant No. 9140C530101130C53013).

†Corresponding author. E-mail: wangfang@mail.xjtu.edu.cn

© 2015 Chinese Physical Society and IOP Publishing Ltd

and the transport of internal charges is required to investigate charge and discharge processes to obtain characteristics of specimen charging states and effects from related sample parameters. As widely used in insulator, protection, and auxiliary materials, polymers are easy to be charged by e-beam because of their high-resistivity property.[18] Here, we take Polymethylmethacrylate (PMMA) as a representative insulation film sample to study its charging characteristics.

In this study, we numerically investigate charge and discharge characteristics of a PMMA film negatively charged due to non-focused e-beam irradiation. The electron scattering procedure in sample considering the emission of SEs is simulated with Monte Carlo method. The transport of charges accumulated in the sample is calculated by the finite-different time-domain (FDTD) method considering drift, diffusion, and trap of internal charges.[10,25] The transient characteristics of internal currents, charge quantity, and surface potential during both charge and discharge processes are then obtained, as well as effects of sample parameters of thickness and electron mobility on charging intensity.

2. Simulation method

We first introduce the simulation model of the charge and discharge formation. Figure 1 shows the schematic of the charge induced by electron irradiation and discharge of PMMA sample. The PMMA film with the thickness H is placed on a grounded basement. The non-focused e-beam irradiates normally to the top surface of the sample. Considering that negative charging of an insulator sample can present more intense surface potential comparing with positive charging, the PMMA film is negatively charged with the surface potential $V_S < 0$[26] by setting the PE energy E_{PE} larger than the secondary cross energy in the curve of SE yeild, which is about 2.1 keV for PMMA material.[27]

Based on the continuity of electric current, the inflow current (PE current J_{PE}) and outflow currents (SE current J_{SE} and sample current J_S), satisfy J_{PE}=$J_{SE}+J_S$. J_S obtained at the grounded bottom is constituted with the leakage current J_L resulted by internal charge transport and the displacement current J_D due to the induced electric field. The accumulated charges will be released in the form of leakage current J_L towards the grounded basement under the force of internal built-in E-field.[28] When the quantity of internal charges in the sample reaches saturation, the displacement current J_D disappears, so the electron currents balance as J_{PE}=$J_{SE}+J_L$. To acquire complete charging characteristics during charge and discharge processes, the discharge process starts once the e-beam irradiation stops ($J_{PE}=0$). Accordingly, the charge process during electron irradiation consists of electron scattering and charge transport, while the discharge process only deals with charge transport after the irradiation. The electron scattering and transport processes are simulated in sequence because the former is much faster than the later.[19]

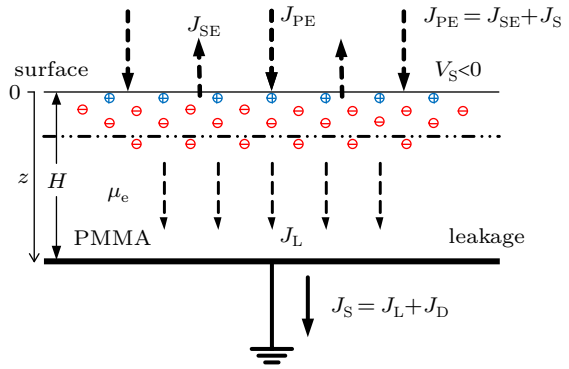


Fig. 1. (color online) Schematic of electron irradiation on the grounded PMMA film with the electron mobility μ_e and thickness H. J_{PE}, J_{SE}, J_S, J_L, and J_D are the PE current, SE current, sample current, leakage current, and displacement current, respectively.

2.1. Electron scattering model

Electron scattering in PMMA, including the elastic and inelastic scattering, are simulated with the Monte Carlo method. In this simulation, the PE energy is set to be less than 10 keV. The Mott cross-section[29] is adopted to describe the elastic scattering as

$$\frac{\mathrm{d}\sigma}{\mathrm{d}\Omega} = |f(\theta)|^2 + |g(\theta)|^2, \tag{1}$$

where σ is the Mott scattering cross-section, Ω and θ are solid angle and scattering angle, $f(\theta)$ and $g(\theta)$ denote the incident and the scattering wavelength division functions, respectively. Considering the complexity of calculating the Mott differential scattering cross section, we use the Mott scattering cross-section database[30] for different sample atoms, PE energy, and scattering angles. The total elastic scattering cross section can be obtained by

$$\sigma_T = 2\pi \int_0^{\pi} \frac{\mathrm{d}\sigma}{\mathrm{d}\Omega} \sin\theta \,\mathrm{d}\theta. \tag{2}$$

The inelastic scattering cross section σ_{in} is calculated with the fast secondary electron model[31] when the PE energy E_{PE} is larger than 3 keV

$$\begin{aligned}\sigma_{in} &= \int_{\theta_c}^{0.5} \left(\frac{\mathrm{d}\sigma}{\mathrm{d}\Omega}\right)_M \\ &= \frac{\pi e^4}{E^2}\left\{\frac{1}{\Omega^2} + \frac{1}{(1-\Omega)^2} + \ln\left(\frac{\Omega_c}{1-\Omega_c}\right)\right\},\end{aligned} \tag{3}$$

in which E is the incident electron energy, e denotes the absolute value of the electron charge, and Ω_c is the minimum of normalized energy loss coefficient and set to be 0.001. The energy loss of inelastic scattering events is calculated with the modified Bethe energy loss formula by Joy and Luo[31]

$$\left(\frac{\mathrm{d}E}{\mathrm{d}S}\right)_{\text{Bethe}} = 78500\frac{\rho\bar{Z}}{\bar{A}E}\ln\left(\frac{1.166(E+k\bar{J})}{\bar{J}}\right), \tag{4}$$

where the coefficient k is interpolated with the average atmospheric atom number $\bar{Z}$, $\bar{A}$ and $\bar{J}$ are the average atomic weight

and the average ionization energy, respectively, and ρ is the density of material.

When E_{PE} is less than 3 keV, the inelastic scattering of electrons is more suitable to be calculated with the Penn model.[32] The corresponding inelastic differential cross section is represented by

$$\frac{\mathrm{d}\lambda_{in}^{-1}}{\mathrm{d}(\Delta E)} = \frac{1}{\pi a_0 E_{PE}} \int_0^{\infty} \frac{E_p \mathrm{d}E_p}{\Delta E^2 - E_p^2 + \left(\frac{(\hbar\bar{q})^2}{2m}\right)^2} \times \mathrm{Im}\left(\frac{-1}{\varepsilon(E_p)}\right) \Theta\left(\frac{\hbar^2}{2m}(2k\bar{q} - \bar{q}^2) - \Delta E\right), \quad (5)$$

where λ_{in} is the electron mean free path of inelastic scattering, Θ is the staircase function considering conservation of energy and momentum, ΔE is the electron transfer energy, E_p is plasma energy satisfying $E_p = \hbar\omega_p$, with ω_p being plasma frequency, a_0 is the Bohr radius, $k = \sqrt{2mE}/\hbar$ is the electron free wave vector, $\bar{q}$ is the root of the following dispersion equation:

$$\omega^2 = \omega_p^2 + \frac{1}{3}v_F^2\bar{q}^2 + \left(\frac{\hbar\bar{q}}{2m}\right)^2, \quad (6)$$

where v_F is the Fermi velocity. When the energy loss during each inelastic scattering event is larger than the band gap of material, an SE will be generated, leaving a hole in the sample. The SE will travel in the sample like a PE until it exhausts its energy or escapes from the sample surface.

Due to the elastic and inelastic scattering, some electrons deposit in the sample, while others can escape as the SEs.[33] To verify the electron scattering model for PMMA, the SE yield δ defined as the ratio of the number of SEs to the number of PEs, $\delta = N_{SE}/N_{PE}$, is calculated and compared with experimental results. As shown in Fig. 2, the simulated δ depicted by a solid line for a PMMA sample with the flat surface is presented as a function of primary energy E_{PE}, compared with the experiment result from Boudaya and Blaise.[27] Under the same neutrality surface potential, the agreement between simulation and experiment is obtained.

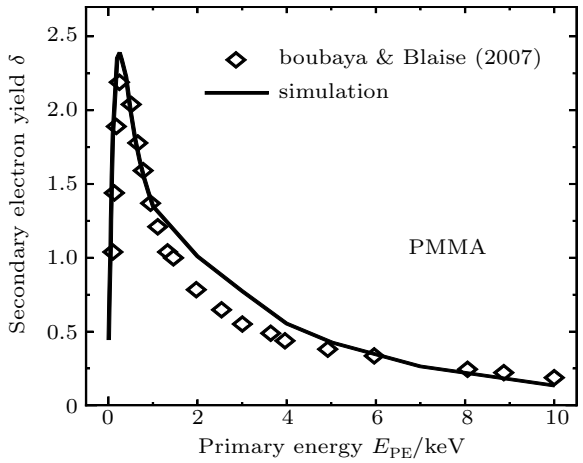


Fig. 2. Secondary electron yield δ as a function of primary energy E_{PE}. Experiment results are plotted for comparison.

2.2. Transport model

The charge transport, including both the charge drift and diffusion caused by the build-in electric field and charge density gradient, are both taken into consideration in the charge and discharge processes. During the transport, some of the deposited charges may be trapped by trapping centers which widely exist in polymer materials.[34] The transport of holes are neglected for their low volume and velocity on charging.[19]

During the charge process, the variation of free electron density $n_F(t)$ in the sample with time t satisfies

$$\frac{\partial n_F}{\partial t} = \left(\frac{\partial n_F}{\partial t}\right)_{scat} + \left(\frac{\partial n_F}{\partial t}\right)_{drift} + \left(\frac{\partial n_F}{\partial t}\right)_{diff} + \left(\frac{\partial n_F}{\partial t}\right)_{trap}, \quad (7)$$

where terms with subscripts scat, drift, diff, and trap represent internal electrons distributions, drift, diffusion, and trap, respectively. The term $(\partial n_F/\partial t)_{scat}$ in the charge process is calculated with the Monte Carlo method mentioned above according to different energies of irradiation electron. The landing energy of PEs is modified by the sample surface potential $E_{land} = E_{PE} - |V_S|$. Other terms in Eq. (7) satisfy

$$\left(\frac{\partial n_F}{\partial t}\right)_{drift} = \nabla \cdot (\mu_e n_F \boldsymbol{E}_f), \quad (8)$$

$$\left(\frac{\partial n_F}{\partial t}\right)_{dif} = \nabla \cdot (D_e \nabla n_F), \quad (9)$$

$$\left(\frac{\partial n_F}{\partial t}\right)_{trap} = -\frac{n_F}{\tau_F}\left(1 - \frac{n_t}{N_T}\right), \quad (10)$$

where μ_e is the electron mobility of the sample material, $\boldsymbol{E}_f$ is the build-in electric field intensity, D_e is the electron diffusion coefficient which is a function of μ_e in the Nernst-Einstein relation as $D_e = \mu_e k_B T/e$ (k_B is Boltzmann constant and temperature $T = 300$ K), n_t is the density of trapped electrons in trapping center, τ_F is the trap time constant of 1 s, and $N_T = 1.0 \times 10^{15}$ cm^{-3} is the density of trapping center for PMMA, respectively.[18] In addition, the space potential $V(z,t)$ inside the sample is calculated with the Poisson equation due to the sample net charge distribution as

$$\nabla^2 V(z,t) = \frac{-e\,[n_{NET}(z,t)]}{\varepsilon}, \quad (11)$$

where the net charge distribution $n_{NET}(z,t)$ is obtained by considering hole distribution $h(z,t)$, free electron, and trapped electron distributions as $n_{NET}(z,t) = h(z,t) - n_F(z,t) - n_{trap}(z,t)$. The ε is the dielectric constant. The charge quantity per unit area $Q(t_i)$, accumulated in the sample at $0 < t < t_i$ where t_i is any moment in the charge or discharge process, and can be calculated by

$$Q(t_i) = \left|\int_0^{t_i} J_D \mathrm{d}t\right| = \left|\int_0^{t_i} \varepsilon \frac{\partial\left[\nabla V(z,t)|_{z=H}\right]}{\partial t}\mathrm{d}t\right|,$$
$$\text{or } Q(t_i) = \left|\int_0^{H} e\,[n_{NET}(z,t_i)]\,\mathrm{d}z\right|. \quad (12)$$

In the discharge process, since the inflow PEs stop, the term $(\partial n_F/\partial t)_{scat}$ is set to be zero. Hence, according to Eq. (7), the variation of free electron density $n_F(t)$ with time t during the discharge process satisfies

$$\frac{\partial n_F}{\partial t} = \left(\frac{\partial n_F}{\partial t}\right)_{drift} + \left(\frac{\partial n_F}{\partial t}\right)_{diff} + \left(\frac{\partial n_F}{\partial t}\right)_{trap}. \quad (13)$$

The surface potential $V(z,t)$ and the charge quantity $Q(t_i)$ during the discharge process can also be calculated with Eqs. (11) and (12), respectively. During the whole charge and discharge process, the leakage current $J_L(t)$ satisfy the continuity equations $J_L(t) = -e\mu_e n_F(H,t)\nabla V(H,t) + eD_e\nabla n_F(H,t)$, and the displacement current $J_D(t)$ can be calculated with $J_D(t) = \varepsilon\partial(\nabla V(H,t))/\partial t$.

2.3. Simulation procedure

The whole simulation procedure including both charge and discharge processes is shown in Fig. 3. With the interruption of PE irradiation, the discharging process begins from the former charging states. The discharge process finishes with the disappearance of leakage current. Combining the scattering and the transport models, we simulate the evolution of internal currents $J_L(t)$, $J_D(t)$, surface potential $V_S(t)$, and total charge quantity $Q(t)$ of the sample during both the charge and discharge processes. Simulations were carried out with default values of sample parameters as follows: the electron mobility of PMMA $\mu_e = 1.0\times10^{-10}$ cm^2·V^{-1}·s^{-1}, the sample thickness $H = 10$ μm, the value of PE energy and current are set to be $E_{PE} = 10$ keV and $J_{PE} = 50$ nA·cm^{-2}, respectively.

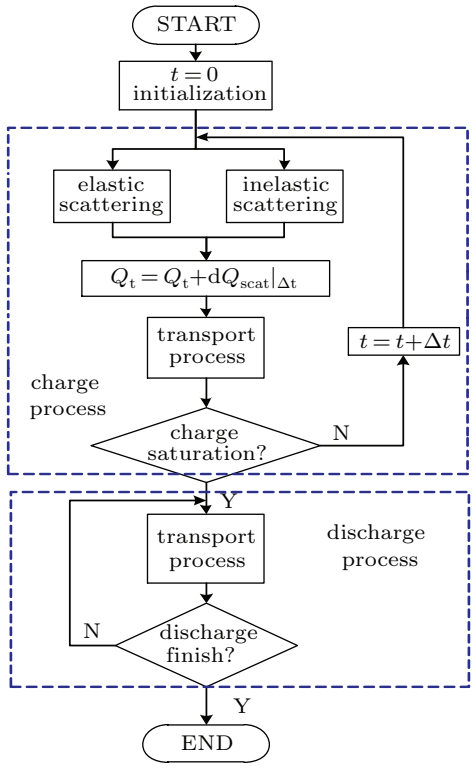


Fig. 3. Solution procedure of charge and discharge processes.

3. Results and discussion

3.1. Transient of charge and discharge

The transient properties of charge and discharge processes of PMMA are presented in Fig. 4. As shown in Fig. 4(a), due to the accumulation of the net inflow charges and the transport of internal charges, the leakage current J_L emerges at 22 s. J_L gradually reaches its maximum and then keeps dynamic balance at 40.5 s. Based on the continuity of electric current, the displacement current J_D appears immediately at the beginning of irradiation. With the emergence and increase of leakage current J_L, J_D gradually reduces to zero when the internal charges accumulated become saturation within the charge duration I as illustrated in Fig. 4(a). In the discharge duration II, when PE irradiation stops, the leakage current J_L gradually decreases to zero with the elapse of internal free charges. The displacement current J_D drops to its negative maximum immediately at the very beginning of discharge duration and then gradually approaches zero, for the continuity of electric current as $J_L + J_D = 0$. The discharge time T_C is defined as the duration from the beginning of discharge t_0 to the moment that leakage current J_L reaches 1% of its maximum t_1 in the discharge process, $T_C = t_1 - t_0$. Here, T_C is ~ 73.1 s according to this calculation.

Due to variations of inflow and outflow currents, the charge quantity and surface potential of the sample will also change. According to Eq. (12), the charge quantity Q_t can be integrated by displacement current J_D. As shown in Fig. 4(b), the quantity of Q_t increases with time t of irradiation until reaches its charging saturation Q_{charge} at the moment when J_L reaches saturation in the charge process. In the discharge process, Q_t decreases gradually to the final value Q_F. Since the de-trap process of trapped charges is negligible for its low volume and speed, the final internal charges Q_F in the discharge process is mainly composed of trap electrons. Accordingly, the discharge quantity in the form of leakage current J_L can be calculated as $Q_{disc} = Q_{charge} - Q_F$. The ratio of discharge quantity r_{dis} defined as $r_{dis} = Q_{disc}/Q_{charge}$, is 0.63 according to the results in Fig. 4(b). Moreover, in the charge process, with the increase of internal charges Q_t, the value of surface potential V_S decreases and keeps a minimum V_{SC} when Q_t reaches saturation. When the electron irradiation stops, V_S increases to its final value V_{SF} which is determined by Q_F.

Figure 5 shows the distribution of sample internal charges in the z direction at different moments during the charge and discharge processes. Due to the drift, diffusion and trap, internal charges transport towards the sample bottom. The position of the maximum charge density related with electron scattering changes slightly in the charge process, as represented by dashed lines, in 11 s, 22 s, and 34 s. However, the maximum

charges density decreases significantly and moves towards the sample bottom in the discharge process. With leakage of free charges in the discharge process, from the moment of 45 s to 88 s, the internal charge density decreases and finally approach an uniform distribution with the value of trapping center $N_T = 1.0 \times 10^{15}$ cm^{-3}.

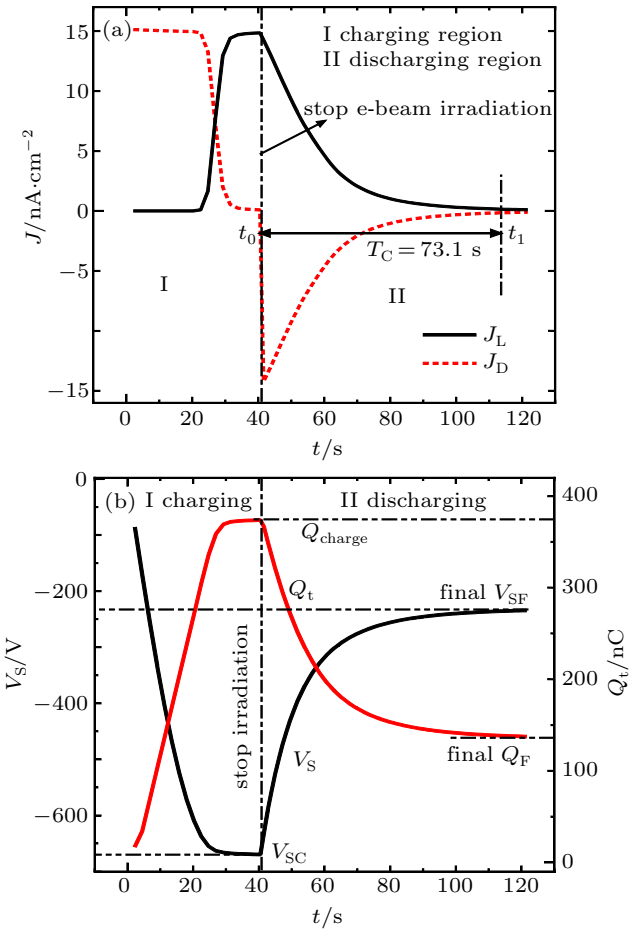


Fig. 4. (color online) Transient characteristics of charge and discharge processes of the PMMA sample. (a) Variations of leakage current J_L and displacement current J_D with time t. T_C is the discharge time. (b) Variations of internal charge quantity Q_t and surface potential V_S with time t.

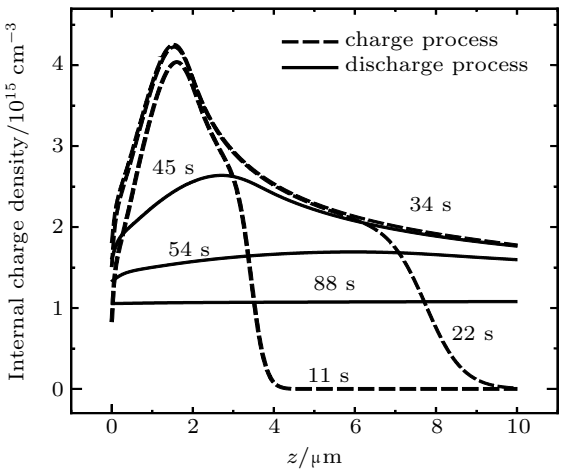


Fig. 5. Internal charge distributions in the z direction at different times.

3.2. Effect of sample thickness

We also simulate the charge and discharge processes for the PMMA sample of different thicknesses. The sample thickness H is 4–20 μm, widely used as a cover film. Figure 6(a) presents the negative charge quantity Q and surface potential V_S, as functions of H. The charge quantity in saturation Q_{charge} and discharge quantity Q_{disc} increases with the increase of H. Q_{charge} is composed of trapped electrons and free electrons in the sample. Q_{disc} is almost from free electrons. As reported in our previous work,[25] the quantity of trapped electrons increase almost linearly with the increase of H, while the increase of free electrons with H is more slowly. Therefore, the increase of the sample thickness H results in more increase in Q_{charge} than in Q_{disc} as shown in Fig. 6(a). The discharge quantity ratio r_{dis} then decreases with sample thickness H, as shown in Fig. 6(b).

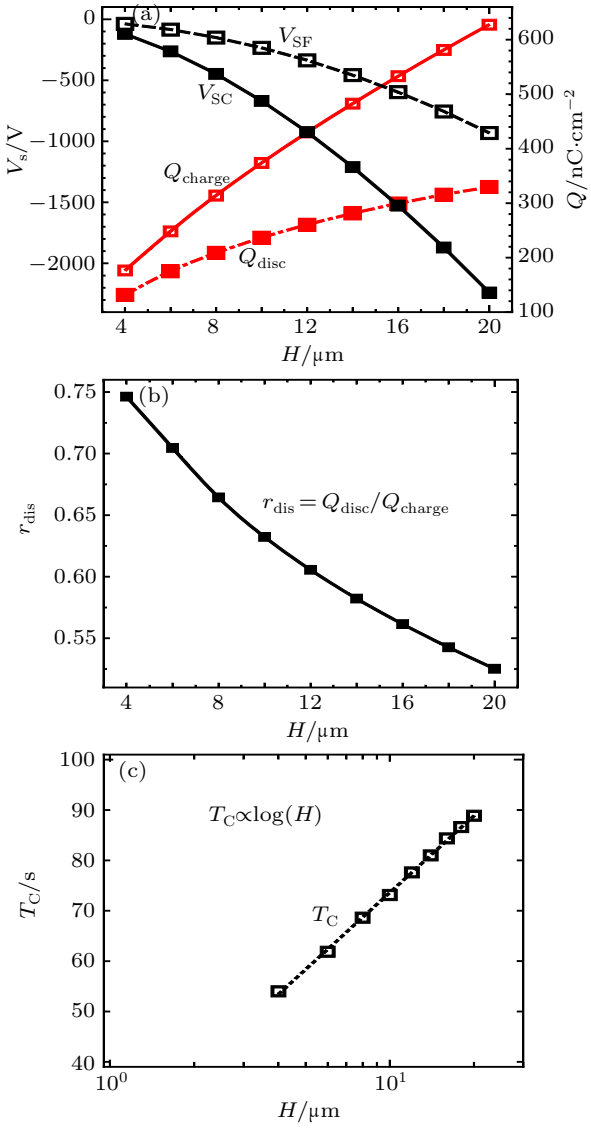


Fig. 6. (color online) (a) Surface potential V_S and charge quantity Q. (b) Discharge ratio r_{dis} and (c) discharge time constant T_C, as functions of the sample thickness H during charge and discharge processes.

Moreover, as illustrated in Fig. 6(a), the surface potential in saturation V_{SC} and surface potential in final state of discharge V_{SF} decrease with the increase in H. The surface potential of the sample is stronger for thicker samples. Meanwhile, the difference between the surface potential in charging saturation V_{SC} and in final state of discharge V_{SF}, which is determined by discharge quantity Q_{disc}, increases with the increase in H.

As shown in Fig. 6(c), in thicker sample, free electrons need longer T_C to leak to the grounded basement due to longer paths during the discharge process. The simulation results also show that the time constant T_C increase with the increase of sample thickness H logarithmically as $T_C \sim \log(H)$.

3.3. Effect of electron mobility

The charge and discharge properties are also affected by electron mobility μ_e of the sample. For PMMA, μ_e can vary from 10^{-9} to 10^{-11} $cm^2 \cdot V^{-1} \cdot s^{-1}$.[18,19] Figure 7(a) shows that the charge quantity in saturation Q_{charge} and the discharge quantity Q_{disc} decrease with the increase of μ_e almost in the same amount. Larger electron mobility μ_e makes free electrons leakage faster in the sample, which results in a less free charge quantity in charging saturation. Hence, both Q_{charge} and Q_{disc} decrease with μ_e, and the surface potential in saturation V_{SC} determined by Q_{charge} increase with μ_e. Since the difference between Q_{charge} and Q_{disc} is mainly composed of trapped electrons, which is independent of μ_e, the difference almost remains constant. Furthermore, the surface potential in the final state of discharge V_{SF} determined by trapped electrons keeps invariable with μ_e.

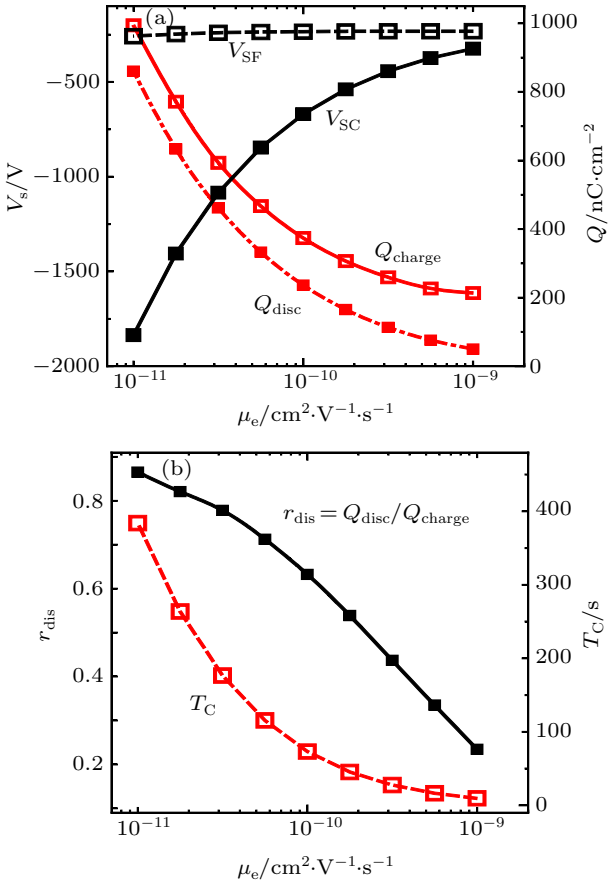


Fig. 7. (color online) (a) Surface potential V_S and total charge quantity Q; (b) discharge ratio r_{dis} and discharge time constant T_C, as functions of the sample electron mobility μ_e during charge and discharge processes.

According to the variations of Q_{charge} and Q_{disc} shown in Fig. 7(a), the discharge quantity ratio r_{dis} decreases with the increase of μ_e, as shown in Fig. 7(b). Since larger electron mobility promotes the transport of free electrons, less time is needed for discharge process to reach its final states. Then, T_C decreases with the increase of μ_e, as illustrated in Fig. 7(b).

It should be noted that the discharge process in this simulation begins immediately after the charging reaches saturation. If the irradiation duration is extended, the charging saturation of sample will remain, and the discharging process after irradiation will be the same. If the interval of irradiation is shorter than the discharge time, the charge quantity and the surface potential of the sample will be stronger. In some cases, in order to weaken the charging effect, e-beam irradiation with an optimum interval estimated by this method is helpful. Moreover, some other parameters, such as trapping center density, temperature and permittivity, will also affect polymer charging.[35–37] Further efforts could adopt this simulation method by taking more factors into account.

4. Conclusion

In summary, we have simulated and analyzed the charge and discharge characteristics of PMMA due to electron irradiation by a numerical simulation. The simulation shows that the charge accumulation by electron irradiation in the sample may reach charge saturation, and then decrease to their final states of discharge in which internal free charges dissipated and trapped electrons almost persist after stopping the electron irradiation. Although both charge and discharge quantities increase with sample thickness, but the discharge quantity ratio is less in a larger thickness sample. A PMMA sample with larger thickness or smaller electron mobility will have a stronger negative surface potential in the charge saturation. The surface potential derived from trapped electrons at the end of discharge is almost independent of electron mobility. Furthermore, the discharge time could decrease logarithmically with the decrease in sample thickness. Effects of sample thickness and electron mobility on the discharge time and the discharge quantity ratio can be considered for weakening charging under the intermittent irradiation. The results presented clarified the charge and discharge characteristics of the PMMA film due to internal charge transport and leakage, and

the simulation method may help to predict the charging states for various samples.

Acknowledgements

We are sincerely indebted to our advisor Dr. H. B. Zhang (deceased), Professor of Xi'an Jiaotong University, for his long-term encouragement and advice.

References

[1] Oatley C W, Nixon W C and Pease R F W 1966 *Adv. Electron. Electron Phys.* **21** 181
[2] Hawkes P W 2012 *Ultramicroscopy* **119** 9
[3] Cazaux J 2010 *J. Electron Spectrosc. Relat. Phenom.* **176** 58
[4] Ciappa M, Koschik A, Dapor M and Fichtner W 2010 *Microelectron. Reliab.* **50** 1407
[5] Cornet N, Goeuriot D, Touzin M, Guerret-Piecourt C, Juve D, Treheux D and Fitting H J 2009 *J. Non-Cryst. Solids* **355** 1111
[6] Ura K 1998 *J. Electron Microsc.* **47** 143
[7] Li W Q and Zhang H B 2010 *Appl. Surf. Sci.* **256** 3482
[8] Xiao P, Zhang Z M, Sun X and Ding Z J 2006 *Acta Phys. Sin.* **55** 5803 (in Chinese)
[9] Zhang H B, Li W Q and Cao M 2012 *J. Electron Microsc.* **61** 85
[10] Cao M, Wang F, Liu J and Zhang H B 2012 *Chin. Phys. B* **21** 127901
[11] Vila F, Sessler G M and Sykja H 2005 *J. Electrost.* **63** 749
[12] Hiro S, Tsuji K and Fujii H 1999 *Electr. Eng. Jpn.* **129** 10
[13] Miyoshi M and Ura K 2005 *J. Vac. Sci. Technol. B* **23** 2763
[14] Czeremuszkin G, Latreche M and Wertheimer M R 2001 *Nucl. Instrum. Meth. B* **185** 88
[15] Babin S, Borisov S and Ivanchikov A 2009 *Proc. SPIE* **7378** 737818
[16] Fakhfakh S, Jbara O and Fakhfakh Z 2009 *Annu. Rep. Conf. Electr. Insul. Dielectr. Phenom.* p. 232
[17] Hillenbrand J, Motz T, Sessler G M, Zhang X, Behrendt N, von Salis-Soglio C, Erhard D P, Altstaedt V and Schmidt H W 2009 *J. Phys. D: Appl. Phys.* **42** 065410
[18] Sessler G M, Figueiredo M T and Ferreira G F L 2004 *IEEE Trans. Dielectr. Electr. Insul.* **11** 192
[19] Sessler G M 1992 *IEEE Trans. Electr. Insul.* **27** 961
[20] Min D M, Li S T, Cho M G and Khan A R 2013 *IEEE Trans. Plasma Sci.* **41** 3349
[21] Qin X G, He D Y and Wang J 2009 *Acta Phys. Sin.* **58** 684 (in Chinese)
[22] Ohya K, Inai K, Kuwada H, Hayashi T and Saito M 2008 *Surf. Coat. Technol.* **202** 5310
[23] Askri B, Raouadi K, Renoud R and Yangui B 2009 *J. Electrost.* **67** 695
[24] Fakhfakh S, Jbara O, Rondot S, Hadjadj A and Fakhfakh Z 2012 *J. Non-Cryst. Solids* **358** 1157
[25] Feng G B, Cao M, Yan L P and Zhang H B 2013 *Micron* **52** 62
[26] Li W Q and Zhang H B 2008 *Acta Phys. Sin.* **57** 3219 (in Chinese)
[27] Boubaya M and Blaise G 2007 *Eur. Phys. J. Appl. Phys.* **37** 79
[28] Huang J G and Chen D 2004 *Acta Phys. Sin.* **53** 961 (in Chinese)
[29] Czyzewski Z, MacCallum D O, Romig A and Joy D C 1990 *J. Appl. Phys.* **68** 3066
[30] http://web.utk.edu/˜srcutk/Mott/mott.htm.
[31] Joy D C 1995 *Monte Carlo Modeling for Electron Microscopy and Microanalysis* (New York: Oxford University Press)
[32] Penn D R 1987 *Phys. Rev. B* **35** 482
[33] Xie A G, Song B and Zhao H F 2008 *J. Anhui University* **32** 3 (in Chinese)
[34] Akbari D, Soltani N and Farahani M 2013 *P. I. Mech. Eng. B-J. Eng.* **227** 430
[35] Liu J and Zhang H B 2014 *Surf Rev Lett* **21** 1450062
[36] Elsafi B, Fakhfakh S, Fakhfakh Z and Jbara O 2011 *Nucl. Instrum. Meth. B* **269** 2715
[37] Zheng F H, Zhang Y W, Xia J F, Xiao C and An Z L 2009 *J. Appl. Phys.* **106** 064105